Hindawi Publishing Corporation
Journal of Nanomaterials
Volume 2013, Article ID 463951, 10 pages
http://dx.doi.org/10.1155/2013/463951

Research Article

Optical Properties and *In Vitro* Biological Studies of Oligonucleotide-Modified Quantum Dots

Valérie A. Gérard,[1] Mark Freeley,[1] Eric Defrancq,[2] Anatoly V. Fedorov,[3] and Yurii K. Gun'ko[1,3]

[1] *School of Chemistry and CRANN, Trinity College Dublin, Dublin 2, Ireland*
[2] *Département de Chimie Moléculaire, UMR CNRS 5250, Université Grenoble Alpes, 38000 Grenoble, France*
[3] *Saint Petersburg National Research University of Information Technologies, Mechanics and Optics, 197101 Saint Petersburg, Russia*

Correspondence should be addressed to Yurii K. Gun'ko; igounko@tcd.ie

Received 9 May 2013; Accepted 14 August 2013

Academic Editor: Pathik Kumbhakar

Water-soluble semiconducting nanocrystals or quantum dots (QDs) have attracted much interest in recent years due to their tuneable emission and potential applications in photonics and biological imaging. Fluorescence resonance energy transfer (FRET) processes are very important for elucidating biochemical mechanisms *in vitro*, and QDs constitute an excellent substrate for this purpose. In this work, new oligonucleotide-functionalised CdTe-based QDs were prepared, characterised and biologically tested. These QDs demonstrated interesting optical properties as well as remarkable *in vitro* behaviour and potential for a range of biological applications.

1. Introduction

Quantum dots (QDs) are semiconductor nanoparticles where the electrons and holes are quantum-confined, which translates into strong photoluminescence (PL) in the visible range. The emission wavelength is directly related to the particle size as larger particles will absorb lower energy, that is, longer wavelength photons [1]. Water-soluble CdTe-based QDs have attracted much interest in recent years for their potential applications in biological imaging especially, which consists in illuminating the cell membrane, the cytoplasm, or selected organelles using a fluorophore [2–14]. Choosing an appropriate combination of staining agents enables one to elucidate cellular structures or mechanisms by visualising them with a fluorescence or confocal microscope. In this area, QDs have a number of advantages over organic dyes. QDs have a continuous absorption spectrum for wavelengths that are shorter than the emission wavelength and a narrow and symmetrical emission which can be tuned to a particular wavelength by changing the particle size. It is therefore possible to excite QDs of various colours with the same source and to spectrally resolve their emissions [15].

The aqueous synthesis of thiol-stabilised CdTe QDs has been reported and optimised over the last years and adapted for different types of ligands [2, 4, 16]. Recently, Tikhomirov and coworkers published a method for producing oligonucleotide-modified CdTe QDs using phosphorothioate-functionalised oligonucleotide sequences [17]. They also demonstrated how the number of strands to be immobilised on a single QD is highly dependent on the QD-binding domain of oligonucleotides as well as the particle diameter. On the other hand, QDs are excellent candidates for the observation of fluorescence resonance energy transfer (FRET) phenomena [1, 17–32] owing to their narrow and symmetrical emission spectra. The sensitive distance dependence of FRET makes it a powerful tool for resolving bio-chemical processes *in vitro* and biosensing [23, 33–41]. In this work, a range of oligonucleotide-modified QDs were produced and fully characterised. The role of hybridisation and melting of double-stranded (ds)-DNA in QD interactions was investigated, and the occurrence of energy transfer was studied with various degrees of spectral overlap between donor and acceptor. Finally, the potential of the

new bionanocomposites for *in vitro* biological imaging was assessed.

2. Materials and Methods

2.1. Materials. The oligonucleotides with the sequences (5′ NH_2-A_{10} TAG GAA TAG TTA TCA (T_6) 3′ and 5′ NH_2-A_{10} TGA TAA CTA TTC CTA (T_6) 3′) were prepared according to standard on-support oligonucleotide synthesis. T6 phosphorothioate tail was prepared by using Beaucage reagent during oxidation steps and 5-amino group was introduced at the last step of DNA synthesis by using the corresponding phosphoramidite C6-amino linker from Eurogentec. Al_2Te_3 was purchased from Cerac Inc. All other chemicals for QD synthesis were purchased from Sigma-Aldrich.

2.2. Synthesis of Oligonucleotide-Modified CdTe QDs. We used a modification of the method developed by Gaponik et al. [16] to produce CdTe QDs stabilised with Thioglycolic acid (TGA). Briefly, cadmium perchlorate hydrate Cd $(ClO_4)_2{\cdot}6H_2O$ (5.5 g) and TGA (1.2 mL) were added to 150 mL degassed Millipore water. The pH of the solution was adjusted to 11 by dropwise addition of a 2 M NaOH solution. 30 μL of 100 μM aqueous solution of oligonucleotide (oligo-1: 5′ NH_2-A_{10} TAG GAA TAG TTA TCA (T_6) 3′ or oligo-2: 5′ NH_2-A_{10} TGA TAA CTA TTC CTA (T_6) 3′) was added to the solution. To 0.5 g of Al_2Te_3 15 mL of H_2SO_4 was added to generate H_2Te gas which then bubbled through the Cd/thiol solution. The resulting nonluminescent solution was then heated under reflux. Once the QDs reached the desired size, the reflux was stopped and different fractions were obtained via size-selective precipitation using isopropanol. The final samples were further purified on a Sephadex-G25 column.

2.3. In Vitro Cellular Assay. HT1080 cells were cultured in a medium (500 mL Minimum Essential Medium (MEM) supplemented with 0.055 g of sodium pyruvate, 5 mL of a solution of penicillin (2 mM) and streptomycin (2 mM), 5 mL of 1 mM gentamicin, and 100 mL of fetal bovine serum (FBS) at 37°C and in a 5% CO_2 atmosphere. Cells were plated in 35 cm^2 glass-bottomed petri dishes (from iBidi) at a final concentration of 10^5 cells per dish and left to adhere overnight. Half of the cell medium was then removed from all dishes and replaced by serum-free medium. Cells were incubated for another 4 hours. QDs were added to a final concentrations of 10^{-7} mol/L in Dulbecco's modified phosphate buffered saline (DPBS) with sodium chloride and magnesium chloride, and cells were incubated for another 4 hours. The QD-containing medium was aspirated out of the dishes and the cells were washed three times with DPBS. The cell cultures were finally imaged using an Olympus FV-1000 confocal microscope.

3. Results and Discussion

Complementary sequences of oligonucleotides bearing a T6 phosphorothioate tail at their 3′end and an amino function at their 5′-end (5′ NH_2-A_{10} TAG GAA TAG TTA TCA (T_6) 3′ and 5′ NH_2-A_{10} TGA TAA CTA TTC CTA (T_6) 3′) were used to synthesise three series of modified QDs. The procedure was adapted from the work of Tikhomirov et al. [17]. A range of QD sizes were thus produced and enabled to interact through DNA hybridising. The optical properties of the new composites were investigated, as well as their behaviour in *in vitro* cell cultures.

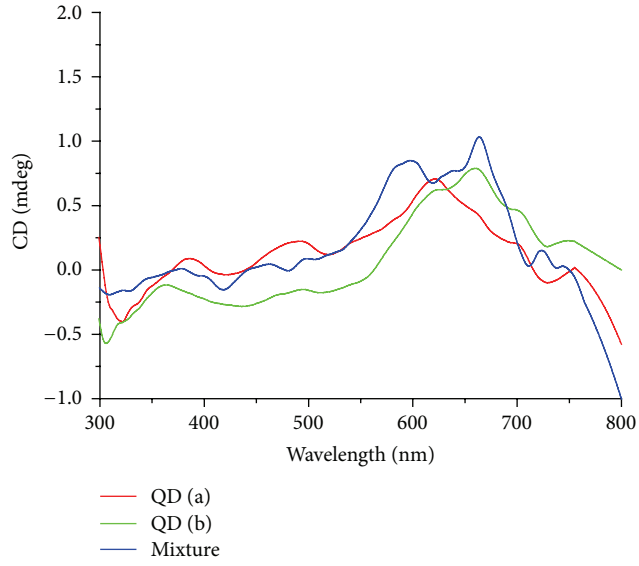

Figure 1: CD spectra of QDs modified with complementary oligonucleotide sequences and their mixture in 1 : 1 ratio.

The presence of oligonucleotides on the surface of QDs and their ability to hybridise with the complementary sequence immobilised on other QDs were confirmed by several instrumental techniques. First, circular dichroism (CD) spectra were recorded for QDs modified with complementary oligonucleotides as well as a one-to-one mixture of those. They exhibited a weak signal in the 500–800 nm range, which corresponds to the position of the exciton peak. The corresponding spectra are shown in Figure 1. It was previously reported that plasmonic nanoparticles may induce CD in that region when a chiral molecule, such as an oligonucleotide, is immobilised on their surface and aggregation occurs [42]. It was also demonstrated that QDs did not produce such an effect when oligonucleotides were coupled to the TGA ligand [42]. In the present case, however, oligonucleotides were bound directly to the surface of QDs, which allowed for closer interactions. The T6 phosphorothioate tail was assumed to lay on the surface, and as a result, the chiral moiety was in direct contact with the particle surface. When bound to the ligand, however, electrostatic repulsion between the carboxylic acid groups and the DNA backbone prevented such contact. Furthermore, it may be assumed that CD signal was generated through local chiral distortion of the crystal structure by chiral ligands, such as previously demonstrated for penicillamine-stabilised CdS and CdSe QDs [43–45]. The CD signal was also not significantly altered by the mixing of complementary-modified

Table 1: Characterisation of oligonucleotide-modified QDs.

Sample	Oligonucleotide	Absorption (nm)	Emission (nm)	Quantum yield	Diameter (nm)	Zeta potential (mV)
Donor (a)	Oligo-2	525	558	27%	2.7	−44
Acceptor (a)	Oligo-1	556	592	25%	3.7	−29
Donor (b)	Oligo-1	535	560	50%	2.9	−35
Acceptor (b)	Oligo-2	601	644	51%	5.2	−40
Donor (c)	Oligo-2	531	567	6%	2.9	−47
Acceptor (c)	Oligo-1	556	592	25%	3.7	−29

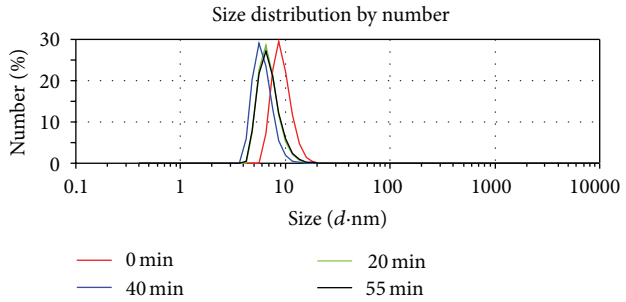

Figure 2: DLS measurements of a 1 : 1 mixture of QDs modified with complementary oligonucleotide sequences and incubated for 0 to 55 min.

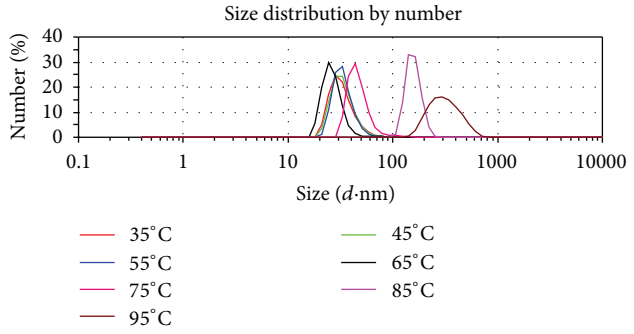

Figure 3: DLS measurements of a 1 : 1 mixture of QDs modified with complementary sequences of oligonucleotides at increasing temperatures.

QDs, thus confirming the predominant role of surface fragments.

For further assessment of the binding effect of oligonucleotides, a 1 : 1 mixture of QD-oligo 1 and QD-oligo 2 was scanned by dynamic light scattering (DLS) in order to measure the changes of the hydrodynamic diameter over time. Figure 2 displays the graph of hydrodynamic diameter distribution from 0 to 55 min of incubation.

The initial mixing of both types of QDs resulted in an average diameter of around 10 nm with a polydispersity index (PDI) of 0.431. As incubation time was prolonged, the PDI did not significantly vary; the average diameter, however, slightly decreased to around 7 nm after 20 min and remained in that range afterwards. This indicated that QDs in initial clusters which were formed in the first 20 min interacted more stronger than and packed more tightly with time. The cluster size of 7 nm was consistent with dimeric structures. Subsequently, the role of oligonucleotide hybridisation in the process was ascertained by measuring the hydrodynamic diameter of the same one-to-one mixture with increasing temperature. Results are displayed on Figure 3. For temperatures up to 65°C, the cluster size fluctuated between 10 and 35 nm while the PDI rose to 0.510 on average. These two effects were mainly imputable to thermal agitation. Further heating, however, led to a dramatic increase in average diameter. The measured values were 41 (±5) nm at 75°C, 174 (±15) nm at 85°C and 326 (±50) nm at 90°C. It was therefore concluded that the nanoclusters dissociated when the temperature was higher than the oligonucleotides melting temperature. The QDs moved further apart but remained grouped together as there was no mechanical agitation. Diffusion would lead over time to a reduction in measured size as QDs could eventually be seen as individual particles. The experiment also demonstrated that hybridisation was possible at physiological temperature (37°C), which is important for potential biological applications.

Having ensured the presence and hybridisation ability of complementary oligonucleotides on QD surfaces, we investigated the energy transfer processes in the nanocomposites. Three sets of donor-acceptor pairs were considered. Their full characterisation data are summarised in Table 1.

In the first pair, the donor emission and acceptor absorption perfectly overlapped which was expected to produce very efficient energy transfer. In the second case, the PL emissions were well separated which enabled good discrimination between them. In the third pair, there was near complete overlap between both absorption and emission spectra, allowing for mutual energy transfer. In each pair, the donor and acceptor were functionalised with oligonucleotide sequences complementary to each other.

Energy transfer in each donor-acceptor pair was investigated by measuring the PL emission of various donor-acceptor solutions of different compositions. The donor quenching and acceptor enhancement were plotted against the donor-to-acceptor ratio (Figures 4–6). The donor quenching is defined as the ratio of the donor intensity in the mixed solution to that of the pure donor at the same concentration. Similarly, the acceptor enhancement is defined as the ratio of the acceptor intensity in the mixed solution to that

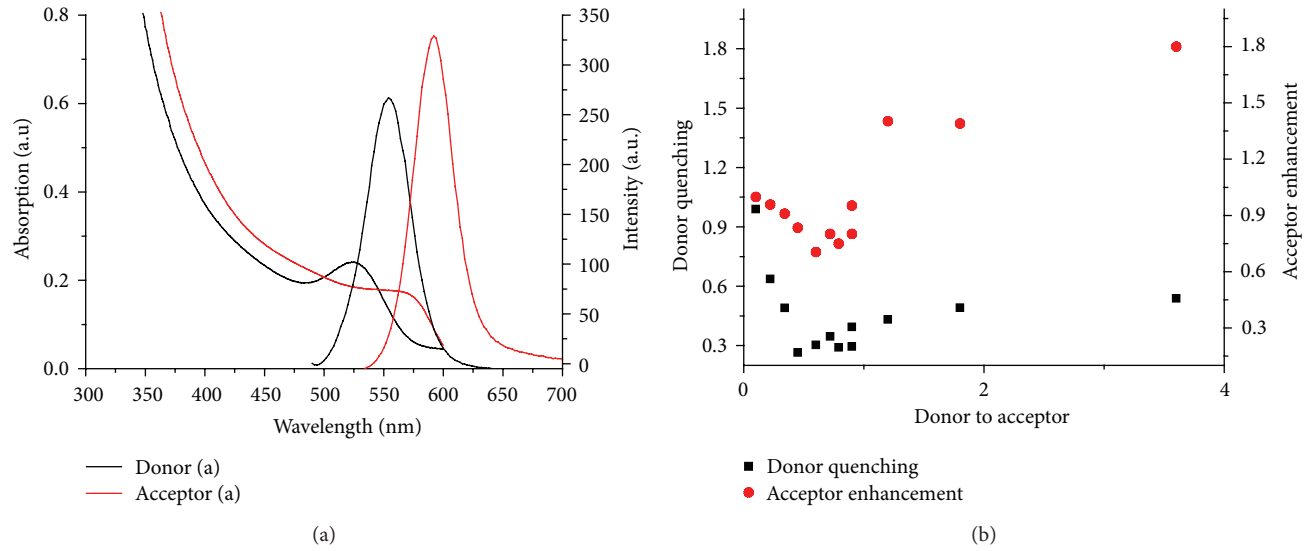

Figure 4: (a): Donor (a) and acceptor (a) UV-visible absorption and PL emission spectra. (b): Donor (a) quenching and acceptor (a) enhancement versus donor-to-acceptor ratio.

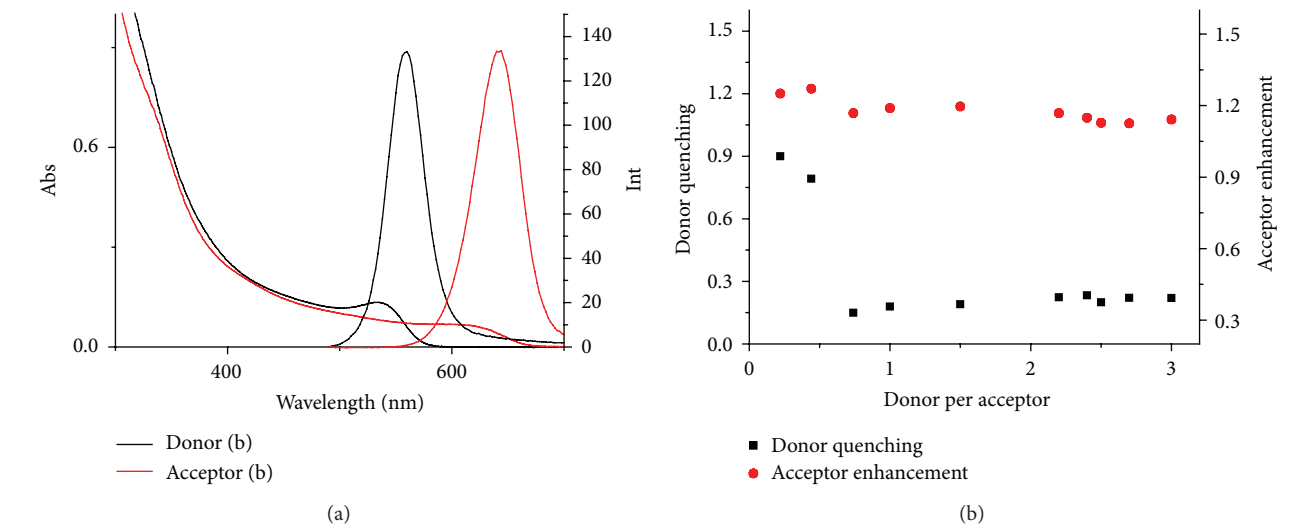

Figure 5: (a): Donor (b) and acceptor (b) UV-visible absorption and PL emission spectra. (b): Donor (b) quenching and acceptor (b) enhancement versus donor-to-acceptor ratio.

of the pure acceptor at the same concentration. It should be noted that donor and acceptor QDs can bind to each other in multiple configurations through oligonucleotide hybridisation and that the complementary domain is approximately 5 nm in length (15 base pairs) [46]. In Tikhomirov et al. work [17], the valency of oligonucleotide-modified QDs was measured for QDs prepared with the same method that was followed here. It was shown to depend on the length of the QD-binding domain of the oligonucleotide and the QD diameter. In our case, the QD-binding domain was a T6 tail; therefore, all QDs are estimated to have a valency of two to three for the donors and three to four for the acceptors. In the first pair (donor (a)–acceptor (a)), as shown in Figure 4, the donor was rapidly quenched for ratios up to 0.5 : 1 where it reached 30% of the original value and remained stable for ratios up to 1 : 1. When the acceptors was in excess, all donor QDs could be assumed to bind to acceptor QDs and to be quenched by them. For these lower ratios, clusters of one donor and two or more acceptor could also form. It led to a slight degree of acceptor quenching through acceptor-to-acceptor intraensemble energy transfer due to spectral overlap of the acceptor absorption and emission. Enhancement of the acceptor PL was thus not observed as long as it was in excess. When the donor-to-acceptor ratio was further increased, the donor emission slightly recovered and plateaued at around 40% of the original value. This was attributed to the possibility of donor-to-donor energy transfer due to partial overlap of donor absorption and donor

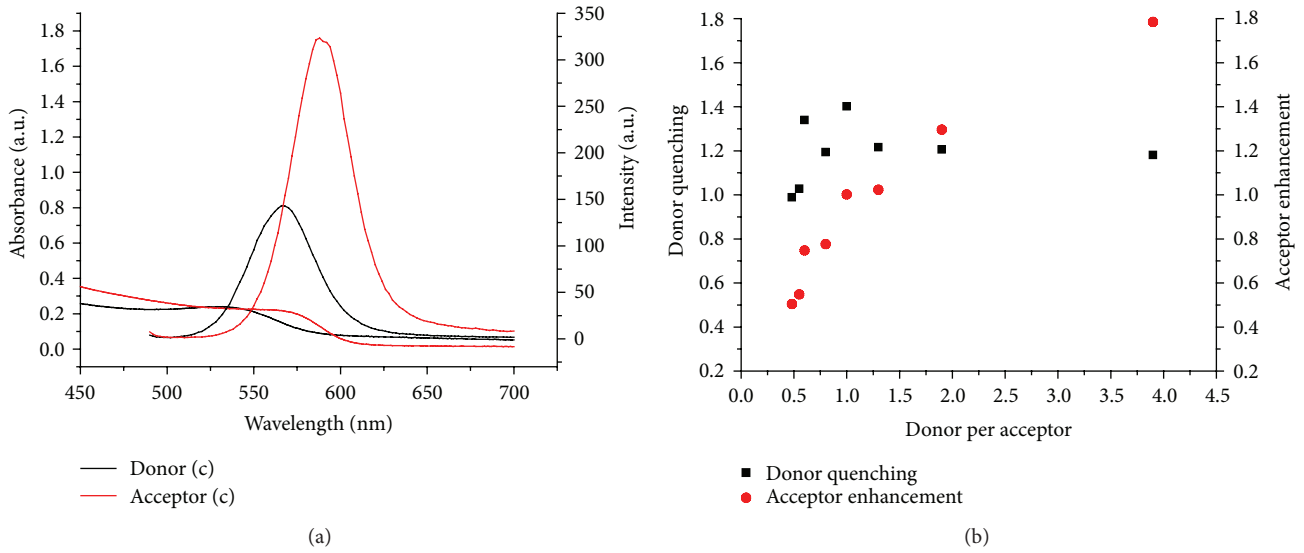

Figure 6: (a): Donor (c) and acceptor (c) UV-visible absorption and PL emission spectra. (b): Donor quenching (c) and acceptor enhancement (c) versus donor-to-acceptor ratio.

emission spectra [18]. Meanwhile, the acceptor emission was gradually enhanced up to 160% of its original value, thus confirming the occurrence of the energy transfer.

Considering the donor-acceptor pair (b) with well-separated absorptions and emissions, the interaction pattern appeared slightly different as presented in Figure 5. At low donor-to-acceptor ratios, a similar trend of rapid donor quenching was observed, down to around 20%. The acceptor emission, however, was immediately enhanced to 120% and remained around that level independently of the amount of donor. The high FRET efficiency at low donor-to-acceptor ratio was due to the high quantum yield of both sets of QDs, while the rapid saturation of the acceptor enhancement was attributed to the spectral separation. As more donor was added its emission slightly recovered due to donor-to-donor intraensemble energy transfer but remained below 50%.

Figure 6 shows that in the pair (c), both sets of QDs had almost completely overlapping spectra. This means that either could actually be donor or acceptor. At low donor-to-acceptor ratio, the so-called "acceptor" was quenched and the "donor" emission was enhanced. The species in excess was most likely to surround the other one through oligonucleotide hybridisation, thus transferring more energy than it received. When the ratio reached one-to-one, the "acceptor" emission had fully recovered, while the donor was still 140% of its original value. It should be noted that the "donor" had a rather low quantum yield of 6% and any energy transfer would therefore translate into a high percentage of variation. Its emission then plateaued at 120% while the acceptor emission continuously rose up to 180% as the donor-to-acceptor ratio was increased. Because of the spectral overlap, it became difficult to distinguish the donor emission at high ratio. It is therefore very likely that the donor was quenched but the emission at that particular wavelength was compensated by the acceptor.

In all cases, energy transfer was observed between QDs modified with complementary oligonucleotide sequences, and there was always a range of ratio for which one was quenched and the other was enhanced. Both donor quenching and acceptor enhancement plateaued between 3 and 4 donors per acceptor, consistently with the calculated valency of the acceptors.

To be suitable for *in vitro* FRET experiments, donor and acceptor must have well-separated emission spectra in order to be detected independently, and FRET should result in nearly full quenching of the donor and maximum enhancement of the acceptor. Only the donor-acceptor pair (b) was found to satisfy these two conditions and was therefore tested in live cell cultures. Two cultures of HT-1080 cells from human fibrosarcoma were incubated with donor (b) and acceptor (b), respectively. Both types of QDs were readily uptaken and could be observed as isolated spots in the cytoplasm, green for the donor and red for the acceptor. A third culture was then incubated with donor and acceptor simultaneously, with no prior mixing. This resulted in the partial colocalisation of donor and acceptor, but isolated green and red QDs could still be seen. Preincubation of donor and acceptor in equal concentrations for an hour and subsequent addition to the cell culture, however, resulted in the donor luminescence completely disappearing and the acceptor emission being enhanced. Thus, our QD-based donor-acceptor system clearly demonstrated fluorescent resonant energy transfer (FRET) inside live HT-1080 cells. Example confocal images of all four types of cultures are displayed in Figure 7. It was therefore concluded that preformed assemblies of QDs persisted in cell cultures but that binding did not spontaneously occur in that biological medium. The disappearance of all green emissions confirmed the occurrence of FRET in the system with near complete quenching of the donor QDs.

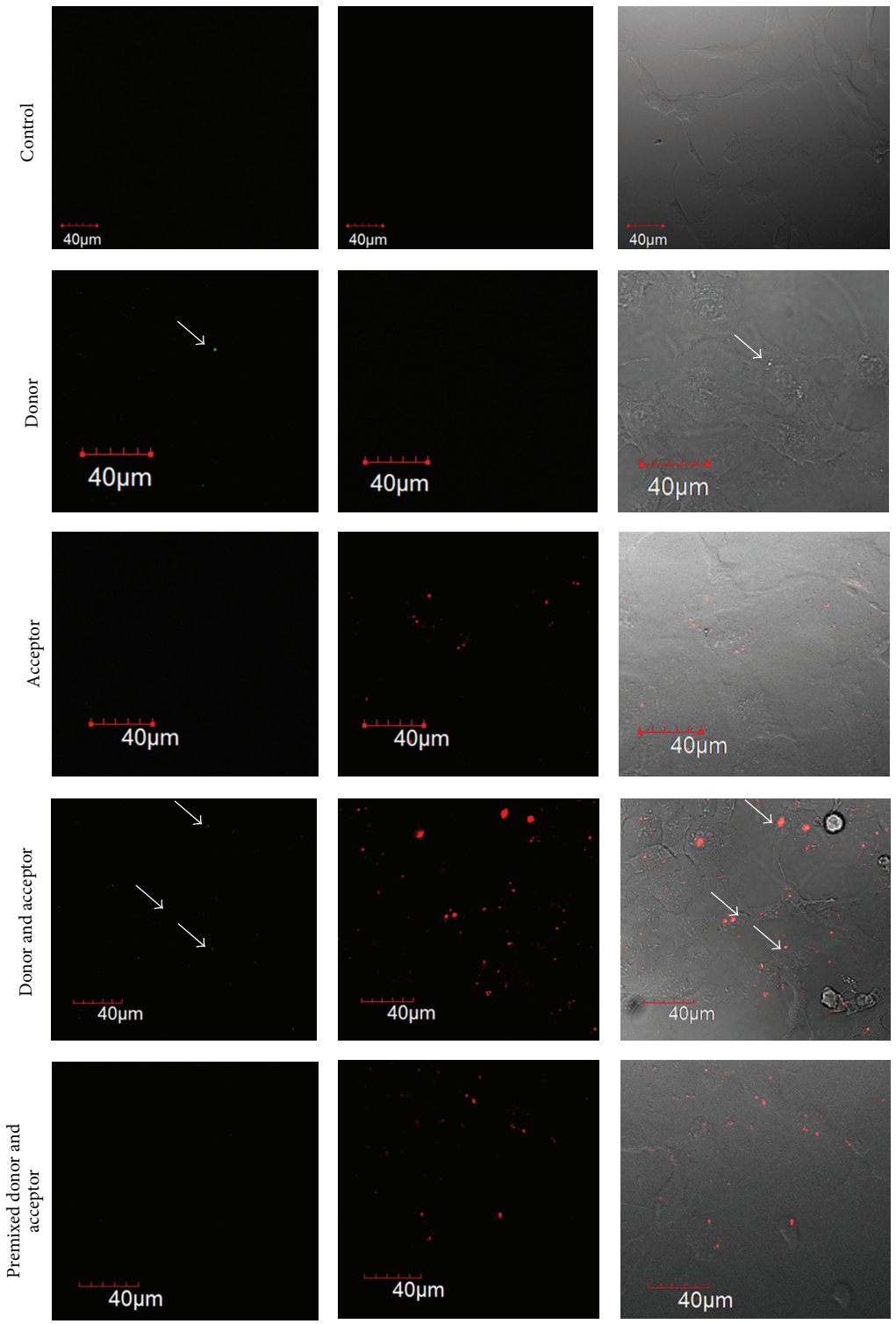

Figure 7: Confocal microscope images of HT-1080 cells exhibiting internalised QDs. First row: negative control; second row: donor (b); third row: acceptor (b); fourth row: donor (b) and acceptor (b) added simultaneously; fifth row: donor (b) and acceptor (b) with preincubation. First column: excitation 543 nm, emission 603 nm; second column: excitation 633 nm, emission 668 nm; third column: overlay of green and red channels with bright field. Arrows indicate green QDs.

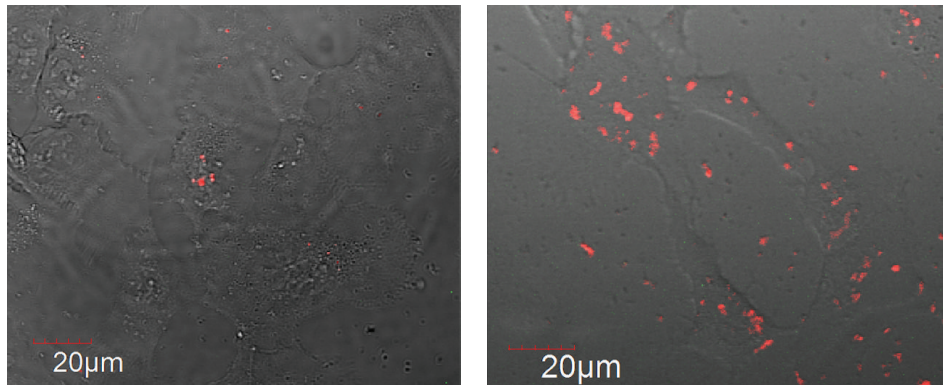

(a) (b)

Figure 8: Confocal microscope close-up images of HT-1080 cells exhibiting internalised green and red QDs. (a) Without preincubation. (b) With preincubation. Overlay of green and red channels with bright field. Excitation 543 nm, emission 603 nm; excitation 633 nm, emission 668 nm.

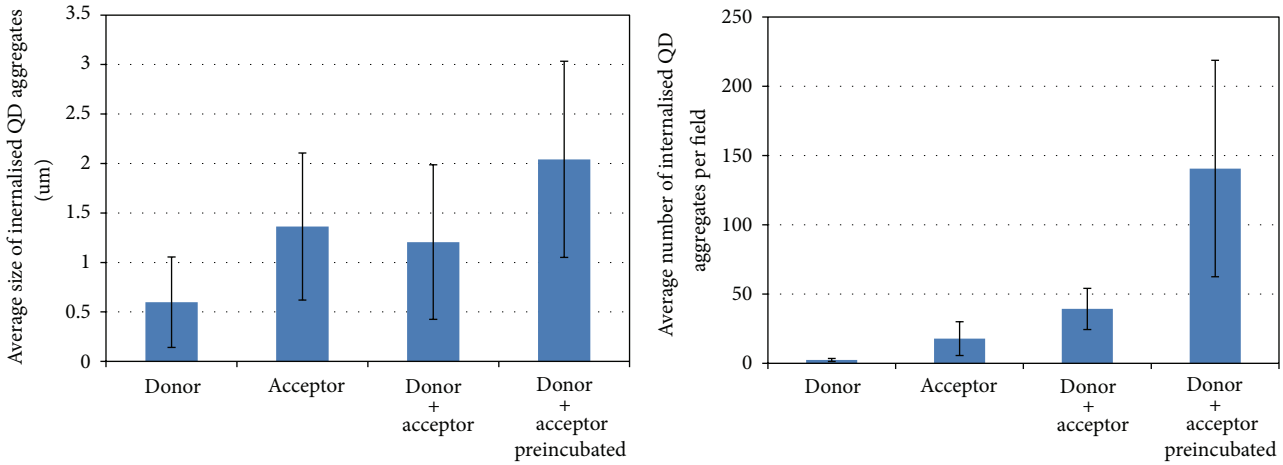

(a) (b)

Figure 9: Histograms representing the number (b) and size (a) of QD aggregates internalised by cells depending on QD type: donor, acceptor, and 1 : 1 mixture with or without preincubation.

Prehybridisation of QDs also resulted in a higher degree of aggregation and accumulation in individual cells as illustrated in Figure 8. This was quantified by both the number and size of QD aggregates visible inside cell cytoplasms and represented in Figure 9. The overall higher internalisation was imputable to the formation of larger aggregates. Larger objects tend to be better internalised by cells due to a thermodynamically favoured attachment to the cell membrane [47].

This observation opened to another possible type of application, where DNA-hybridisation processes could be monitored through QD aggregation using a system where FRET does not occur. Similar cellular testing of the donor-acceptor pair (c) provided an example of such system. As predicted by the fluorescence titration described above, neither species was quenched at 1 : 1 ratio, thus allowing visualising them simultaneously in cells. The presence in cytoplasms of large aggregates containing both red and green QDs confirmed the occurrence of oligonucleotide binding after preincubation. Confocal microscopy images of cells treated with these QDs are displayed in Figure 10.

Thus, the results above demonstrated that our composites were suitable for studying energy transfer processes or DNA binding/digesting processes in cell cultures *in vitro*.

4. Conclusions

In this work, a series of new oligonucleotide-modified CdTe QDs have been prepared, characterized, and tested *in vitro*. Hybridisation and separation of complementary strands of oligonucleotides were assessed as a function of time and temperature. It was found that the hybridised systems demonstrated variable FRET efficiencies depending on spectral overlap, which could be observed *in vitro* in HT-1080 cell cultures. Further work will include an investigation of specific intracellular oligonucleotide-modified QD interactions in various cell cultures to understand and explain the biological behaviour of these nanomaterials in detail. We believe that

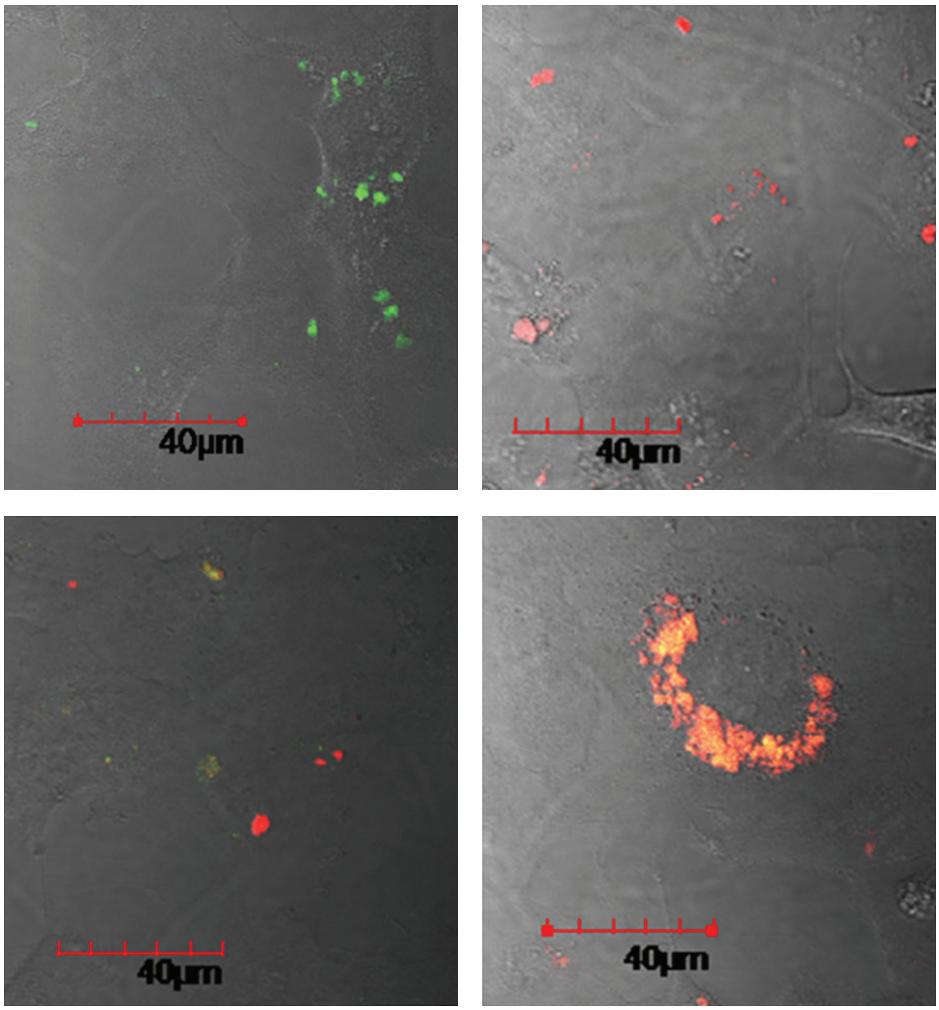

Figure 10: Confocal microscope images of HT-1080 cells exhibiting internalised QDs. (a) donor (c), (b) acceptor (c), (c) donor (c) + acceptor (c) added simultaneously, (D) donor (c) + acceptor (c) after a one-hour preincubation. Overlay of bright field with green and red channels.

these QD-oligonucleotide conjugates might find important applications for *in vitro* biological imaging and sensing.

Acknowledgments

The authors acknowledge financial support from Science Foundation Ireland (Grants SFI 07/IN.1/I1862 and SFI 12/IA/1300) and the Ministry of Education and Science of the Russian Federation (Grant no. 14.B25.31.0002). E. Defrancq thanks the NanoBio program for the facilities of the synthesis platform.

References

[1] D. Ramadurai, D. Geerpuram, D. Alexson et al., "Electrical and optical properties of colloidal semiconductor nanocrystals in aqueous environments," *Superlattices and Microstructures*, vol. 40, no. 1, pp. 38–44, 2006.

[2] S. J. Byrne, S. A. Corr, T. Y. Rakovich et al., "Optimisation of the synthesis and modification of CdTe quantum dots for enhanced live cell imaging," *Journal of Materials Chemistry*, vol. 16, no. 28, pp. 2896–2902, 2006.

[3] J. Conroy, S. J. Byrne, Y. K. Gun'ko et al., "CdTe nanoparticles display tropism to core histones and histone-rich cell organelles," *Small*, vol. 4, no. 11, pp. 2006–2015, 2008.

[4] S. J. Byrne, Y. Williams, A. Davies et al., "'Jelly dots': synthesis and cytotoxicity studies of CdTe quantum dot-gelatin nanocomposites," *Small*, vol. 3, no. 7, pp. 1152–1156, 2007.

[5] E. Jan, S. J. Byrne, M. Cuddihy et al., "High-content screening as a universal tool for fingerprinting of cytotoxicity of nanoparticles," *ACS Nano*, vol. 2, no. 5, pp. 928–938, 2008.

[6] S. J. Byrne, B. Le Bon, S. A. Corr et al., "Synthesis, characterisation, and biological studies of CdTe quantum dot-naproxen conjugates," *ChemMedChem*, vol. 2, no. 2, pp. 183–186, 2007.

[7] M. J. Choi, R. Pierson, Y. Chang, H. Guo, and I. K. Kang, "Enhanced intracellular uptake of CdTe quantum dots by conjugation of oligopeptides," *Journal of Nanomaterials*, vol. 2013, Article ID 291020, 8 pages, 2013.

[8] M. Eriksen, P. Horvath, M. A. Sorensen, S. Semsey, L. B. Oddershede, and L. Jauffred, "A novel complex: a quantum

dot conjugated to an active T7 RNA polymerase," *Journal of Nanomaterials*, vol. 2013, Article ID 468105, 9 pages, 2013.

[9] C. P. Liu, S. H. Cheng, N. T. Chen, and L. W. Lo, "Intra/interparticle energy transfer of luminescence nanocrystals for biomedical applications," *Journal of Nanomaterials*, vol. 2012, Article ID 706134, 9 pages, 2012.

[10] J. Wang, S. Han, D. Ke, and R. Wang, "Semiconductor quantum dots surface modification for potential cancer diagnostic and therapeutic applications," *Journal of Nanomaterials*, vol. 2012, Article ID 129041, 8 pages, 2012.

[11] S. Jin, Y. Hu, Z. Gu, L. Liu, and H.-C. Wu, "Application of quantum dots in biological imaging," *Journal of Nanomaterials*, vol. 2011, Article ID 834139, 13 pages, 2011.

[12] C.-W. Peng and Y. Li, "Application of quantum dots-based biotechnology in cancer diagnosis: current status and future perspectives," *Journal of Nanomaterials*, vol. 2010, Article ID 676839, 11 pages, 2010.

[13] K. Fujioka, N. Manabe, M. Nomura et al., "Detection of thyroid carcinoma antigen with quantum dots and monoclonal IgM antibody (JT-95) system," *Journal of Nanomaterials*, vol. 2010, Article ID 937684, 7 pages, 2010.

[14] S. Mazumder, R. Dey, M. K. Mitra, S. Mukherjee, and G. C. Das, "Review: biofunctionalized quantum dots in biology and medicine," *Journal of Nanomaterials*, vol. 2009, Article ID 815734, 17 pages, 2009.

[15] J. Drbohlavova, V. Adam, R. Kizek, and J. Hubalek, "Quantum dots—characterization, preparation and usage in biological systems," *International Journal of Molecular Sciences*, vol. 10, no. 2, pp. 656–673, 2009.

[16] N. Gaponik, D. V. Talapin, A. L. Rogach et al., "Thiol-capping of CDTe nanocrystals: an alternative to organometallic synthetic routes," *Journal of Physical Chemistry B*, vol. 106, no. 29, pp. 7177–7185, 2002.

[17] G. Tikhomirov, S. Hoogland, P. E. Lee, A. Fischer, E. H. Sargent, and S. O. Kelley, "DNA-based programming of quantum dot valency, self-assembly and luminescence," *Nature Nanotechnology*, vol. 6, no. 8, pp. 485–490, 2011.

[18] C. Higgins, M. Lunz, A. L. Bradley et al., "Energy transfer in colloidal CdTe quantum dot nanoclusters," *Optics Express*, vol. 18, no. 24, pp. 24486–24494, 2010.

[19] A. Gole, N. R. Jana, S. T. Selvan, and J. Y. Ying, "Langmuir-Blodgett thin films of quantum dots: synthesis, surface modification, and fluorescence resonance energy transfer (FRET) studies," *Langmuir*, vol. 24, no. 15, pp. 8181–8186, 2008.

[20] F. Rad, A. Mohsenifar, M. Tabatabaei et al., "Detection of candidatus phytoplasma aurantifolia with a quantum dots fret-based biosensor," *Journal of Plant Pathology*, vol. 94, no. 3, pp. 525–534, 2012.

[21] S. Sadhu, K. K. Haldar, and A. Patra, "Size dependent resonance energy transfer between semiconductor quantum dots and dye using FRET and kinetic model," *Journal of Physical Chemistry C*, vol. 114, no. 9, pp. 3891–3897, 2010.

[22] J. E. Halpert, J. R. Tischler, G. Nair et al., "Electrostatic formation of quantum dot/J-aggregate FRET pairs in solution," *Journal of Physical Chemistry C*, vol. 113, no. 23, pp. 9986–9992, 2009.

[23] F. Long, C. Gu, A. Z. Gu, and H. Shi, "Quantum dot/carrier-protein/haptens conjugate as a detection nanobioprobe for FRET-based immunoassay of small analytes with all-fiber microfluidic biosensing platform," *Analytical Chemistry*, vol. 84, no. 8, pp. 3646–3653, 2012.

[24] F. Morgner, S. Stufler, D. Geißler et al., "Terbium to quantum dot FRET bioconjugates for clinical diagnostics: influence of human plasma on optical and assembly properties," *Sensors*, vol. 11, no. 10, pp. 9667–9684, 2011.

[25] H. Safarpour, M. R. Safarnejad, M. Tabatabaei et al., "Development of a quantum dots FRET-based biosensor for efficient detection of Polymyxa betae," *Canadian Journal of Plant Pathology*, vol. 34, no. 4, pp. 507–515, 2012.

[26] S. Verma, S. Kaniyankandy, and H. N. Ghosh, "Charge separation by indirect bandgap transitions in CdS/ZnSe type-II core/shell quantum dots," *Journal of Physical Chemistry C*, vol. 117, no. 21, pp. 10901–10908, 2013.

[27] T. Ribeiro, T. J. V. Prazeres, M. Moffitt, and J. P. S. Farinha, "Enhanced photoluminescence from micellar assemblies of cadmium sulfide quantum dots and gold nanoparticles," *Journal of Physical Chemistry C*, vol. 117, no. 6, pp. 3122–3133, 2013.

[28] M. Wojdyla, S. A. Gallagher, M. P. Moloney et al., "Picosecond to millisecond transient absorption spectroscopy of broadband emitting chiral CdSe quantum dots," *Journal of Physical Chemistry C*, vol. 116, no. 30, pp. 16226–16232, 2012.

[29] G. Mandal, M. Bardhan, and T. Ganguly, "Occurrence of förster resonance energy transfer between quantum dots and gold nanoparticles in the presence of a biomolecule," *Journal of Physical Chemistry C*, vol. 115, no. 43, pp. 20840–20848, 2011.

[30] C.-H. Wang, C.-W. Chen, C.-M. Wei et al., "Resonant energy transfer between CdSe/ZnS type I and CdSe/ZnTe type II quantum dots," *Journal of Physical Chemistry C*, vol. 113, no. 35, pp. 15548–15552, 2009.

[31] S. M. Emin, N. Sogoshi, S. Nakabayashi, T. Fujihara, and C. D. Dushkin, "Kinetics of photochromic induced energy transfer between manganese-doped zinc-selenide quantum dots and spiropyrans," *Journal of Physical Chemistry C*, vol. 113, no. 10, pp. 3998–4007, 2009.

[32] S. A. Gallagher, S. Comby, M. Wojdyla et al., "Efficient quenching of TGA-capped CdTe quantum dot emission by a surface-coordinated europium(III) cyclen complex," *Inorganic Chemistry*, vol. 52, no. 8, pp. 4133–4135, 2013.

[33] P. R. Selvin, "The renaissance of fluorescence resonance energy transfer," *Nature Structural Biology*, vol. 7, no. 9, pp. 730–734, 2000.

[34] N. T. Chen, S. H. Cheng, C. P. Liu et al., "Recent advances in nanoparticle-based förster resonance energy transfer for biosensing, molecular imaging and drug release profiling," *International Journal of Molecular Sciences*, vol. 13, no. 12, pp. 16598–16623, 2012.

[35] Z. Xia and J. Rao, "Biosensing and imaging based on bioluminescence resonance energy transfer," *Current Opinion in Biotechnology*, vol. 20, no. 1, pp. 37–44, 2009.

[36] D. Geissler, S. Stufler, H. G. Lohmannsroben, and N. Hildebrandt, "Six-color time-resolved Förster resonance energy transfer for ultrasensitive multiplexed biosensing," *Journal of the American Chemical Society*, vol. 135, no. 3, pp. 1102–1109, 2013.

[37] R. Freeman, J. Girsh, B. Willner, and I. Willner, "Sensing and biosensing with semiconductor quantum dots," *Israel Journal of Chemistry*, vol. 52, no. 11-12, pp. 1125–1136, 2012.

[38] E. Petryayeva and U. J. Krull, "Quantum dot and gold nanoparticle immobilization for biosensing applications using multidentate imidazole surface ligands," *Langmuir*, vol. 28, no. 39, pp. 13943–13951, 2012.

[39] W. R. Algar, D. Wegner, A. L. Huston et al., "Quantum dots as simultaneous acceptors and donors in time-gated Förster resonance energy transfer relays: characterization and biosensing,"

Journal of the American Chemical Society, vol. 134, no. 3, pp. 1876–1891, 2012.

[40] C. H. Vannoy, A. J. Tavares, M. O. Noor, U. Uddayasankar, and U. J. Krull, "Biosensing with quantum dots: a microfluidic approach," *Sensors*, vol. 11, no. 10, pp. 9732–9763, 2011.

[41] W. Zhong, "Nanomaterials in fluorescence-based biosensing," *Analytical and Bioanalytical Chemistry*, vol. 394, no. 1, pp. 47–59, 2009.

[42] V. A. Gérard, Y. K. Gun'ko, E. Defrancq, and A. O. Govorov, "Plasmon-induced CD response of oligonucleotide-conjugated metal nanoparticles," *Chemical Communications*, vol. 47, no. 26, pp. 7383–7385, 2011.

[43] M. P. Moloney, Y. K. Gun'ko, and J. M. Kelly, "Chiral highly luminescent CdS quantum dots," *Chemical Communications*, no. 38, pp. 3900–3902, 2007.

[44] S. A. Gallagher, M. P. Moloney, M. Wojdyla, S. J. Quinn, J. M. Kelly, and Y. K. Gun'Ko, "Synthesis and spectroscopic studies of chiral CdSe quantum dots," *Journal of Materials Chemistry*, vol. 20, no. 38, pp. 8350–8355, 2010.

[45] S. D. Elliott, M. P. Moloney, and Y. K. Gun'ko, "Chiral shells and achiral cores in CdS quantum dots," *Nano Letters*, vol. 8, no. 8, pp. 2452–2457, 2008.

[46] C. Rivetti and S. Codeluppi, "Accurate length determination of DNA molecules visualized by atomic force microscopy: evidence for a partial B- to A-form transition on mica," *Ultramicroscopy*, vol. 87, no. 1-2, pp. 55–66, 2001.

[47] X. Li, "Size and shape effects on receptor-mediated endocytosis of nanoparticles," *Journal of Applied Physics*, vol. 111, no. 2, Article ID 024702, 4 pages, 2012.